

# Text Segmentation by Automatically Designed Morphological Operators

NINA S. T. HIRATA, JUNIOR BARRERA AND ROUTO TERADA

Instituto de Matemática e Estatística - USP  
Rua do Matão, 1010  
05508-900 São Paulo - SP - Brazil  
[<nina,jb,rt>@ime.usp.br](mailto:<nina,jb,rt>@ime.usp.br)

**Abstract.** Identification of areas corresponding to text in document images is an important step for a character recognition system. In this paper, we briefly review a technique for automatic design of binary morphological operators and show its application to the segmentation of text areas from document page images. We also present an heuristic filter used to refine the segmentation results. Results obtained for two different sets of images are shown.

## 1 Introduction

Typically, a document image contains objects such as text and figures (diagrams, graphics, half-tones). Information about the localization of these objects in a page image may help document processing systems such as optical character recognition (OCR) systems. The task of separating text from figures is usually composed of two processes : page segmentation and page classification [1]. *Page segmentation* refers to the partitioning of a page image into subregions corresponding to those objects. *Page classification* is the identification of the object type in each region. Several techniques for page segmentation and classification have been proposed. More recent works include [1, 2, 3].

In this paper, we present a novel approach for text segmentation from binary images based on automatically designed binary morphological operators. Automatic design of morphological image operators [4, 5] has been previously applied with success for character recognition [6, 7] and also to other image processing problems. In our approach, a morphological operator is designed for segmenting texts, and its results are further processed by heuristically designed robust morphological filters. The automatically generated segmentation operator plays an important role in the whole segmentation process because its results, even not being perfect, allow a simple post-processing that effectively segments the areas of interest.

Following this, we first review in Section 2 some basic definitions of mathematical morphology for binary images. In Section 3 we recall the automatic design procedure of morphological operators. In Section 4, we present results of the proposed method for several page images, and finally in Section 5 we give the conclusion.

## 2 Elements of Mathematical Morphology

Let  $E = Z^2$  and let  $\mathcal{P}(E)$  denote the power set of  $E$ . Consider also a finite subset  $W \subset E$ , containing the origin  $o$  of  $E$ . The translation of a set  $S \subseteq E$  by a vector  $z \in E$  is denoted  $S_z$  and defined by  $S_z = \{y \in E : y = x + z, x \in S\}$ . The cardinality of a finite set  $S \in \mathcal{P}(E)$  is denoted  $|S|$ . A mapping  $\Psi : \mathcal{P}(E) \rightarrow \mathcal{P}(E)$  is a  $W$ -operator if and only if (iff) it is translation-invariant (i.e.,  $\Psi(S_z) = [\Psi(S)]_z$ , for all  $z \in E$  and  $S \in \mathcal{P}(E)$ ) and locally defined within  $W$  (i.e.,  $x \in \Psi(S) \Leftrightarrow x \in \Psi(S \cap W_x)$ , for all  $x \in E$  and  $S \in \mathcal{P}(E)$ ).

**Proposition 2.1** *A mapping  $\Psi : \mathcal{P}(E) \rightarrow \mathcal{P}(E)$  is a  $W$ -operator iff there exists a mapping  $\psi : \mathcal{P}(W) \rightarrow \{0, 1\}$  such that*

$$x \in \Psi(S) \Leftrightarrow \psi(S_{-x} \cap W) = 1$$

*for all  $x \in E$  and  $S \in \mathcal{P}(E)$ . The mapping  $\psi$  is called the characteristic function of  $\Psi$ .*

The kernel of a  $W$ -operator  $\Psi : \mathcal{P}(E) \rightarrow \mathcal{P}(E)$ , characterized by a function  $\psi$ , is the collection  $\mathcal{K}(\Psi) = \{X \in \mathcal{P}(W) : \psi(X) = 1\}$ . In order to design a  $W$ -operator, one only needs to design its characteristic function, or specify its kernel.

$W$ -operators can be used for binary image processing because binary images can be regarded as subsets of the image domain (in our case, the set  $E$ ). Some operators of mathematical morphology for binary images are presented in the remaining of this section.

**Definition 2.1** *Let  $B \in \mathcal{P}(W)$ . The  $W$ -operators  $\delta_B$  and  $\varepsilon_B$  defined by*

$$x \in \delta_B(S) \Leftrightarrow S \cap B_x \neq \emptyset$$

and

$$x \in \varepsilon_B(S) \iff B_x \subseteq S$$

for any  $x \in E$  and  $S \in \mathcal{P}(E)$ , are called, respectively, dilation and erosion by  $B$ . The set  $B$  is called a structuring element.

**Definition 2.2** The operators  $\gamma_B$  and  $\varphi_B$  from  $\mathcal{P}(E)$  to  $\mathcal{P}(E)$ , given by

$$\gamma_B = \delta_B \varepsilon_B$$

and

$$\varphi_B = \varepsilon_B \delta_B,$$

are called, respectively, opening and closing by  $B$ .

Intuitively, one might think of an opening as the operator that removes objects or part of the objects that are smaller than the structuring element, while closing is the operator that fills spaces between the objects that are smaller than the structuring element.

**Definition 2.3** Given  $k > 0$ , the  $W$ -operator defined by the characteristic function  $\psi(X) = 1 \iff |X| \geq k$ , for all  $X \in \mathcal{P}(W)$ , is the  $k$ -order filter. If  $k = \lceil |W|/2 \rceil$  then it is a median filter.

Let  $S \in \mathcal{P}(E)$  and let  $S^c$  denote the complement of  $S$ . A *hole* of an image  $S$  is any finite connected component of  $S^c$  (in practice, any connected component of  $S^c$  that does not touch the border of the image). The *closing of holes* is an operator that fills all holes of an image. Let  $a > 0$ . An image operator that removes all components of an image with size smaller than  $a$  is called the  $a$ -area open filter. This filter is useful for removing small objects from an image. Formal definitions of these operators can be found, for instance, in [8, 9].

A  $W$ -operator  $\Psi$  is anti-extensive iff  $\Psi(S) \subseteq S$ , for all  $S \in \mathcal{P}(E)$ . For further details on mathematical morphology the reader may refer to [10, 11, 12].

### 3 Automatic Design of Morphological Operators

In general, the approaches to design morphological operators consider descriptions of the desired image transformation given in high-level of abstraction. These descriptions are translated into a specification of a morphological operator that realizes the described transformation. The approach in this paper [4, 5] considers pairs of observed-ideal images, like those shown in Fig. 1, as a description of the desired transformation.

The pairs of observed-ideal images  $(S, I)$  are considered as realizations of random processes  $\mathbf{S}$  and  $\mathbf{I}$ ,



Figure 1: A training pair of observed-ideal images.

and the operators are regarded as estimators of  $\mathbf{I}$  in terms of  $\mathbf{S}$  [13]. In other words, one would like to find an operator  $\Psi$  such that  $\Psi(\mathbf{S})$  is as close as possible to  $\mathbf{I}$ , according to some error measure. Usually, the error measure to be minimized is the mean absolute error, i.e.,  $MAE(\Psi) = E[|\Psi(\mathbf{S})(z) - \mathbf{I}(z)|]$ . Under the assumption that the processes  $\mathbf{S}$  and  $\mathbf{I}$  are jointly stationary, point  $z$  is arbitrary. Hence, they can be characterized by a joint process  $(\mathbf{X}, \mathbf{y})$  where realizations of  $\mathbf{X}$  are subsets of  $W$  and realizations of  $\mathbf{y}$  are in  $\{0, 1\}$ . The measure to be minimized is then written as  $MAE(\Psi) = E[|\psi(\mathbf{X}) - \mathbf{y}|]$ . Given the probabilities  $P(X) = P(\mathbf{X} = X)$  of observing  $X$  and the conditional probabilities  $p(1|X) = P(\mathbf{y} = 1|X)$  of observing value 1 in the ideal image given that pattern  $X$  has been observed in the observed image, the MAE-optimal  $W$ -operator is characterized by the function:

$$\psi_{opt}(X) = \begin{cases} 1, & \text{if } p(1|X) > 0.5, \\ 0, & \text{if } p(1|X) \leq 0.5. \end{cases} \quad (1)$$

In practice, in order to estimate the optimal operator, sample pairs of observed-ideal images are used to estimate the conditional probabilities  $p(1|X)$ . Some patterns  $X \in \mathcal{P}(W)$  may not be observed in the sample and therefore the value of the operator stays undefined for those patterns. Moreover, the representation of the operator by means of its kernel is not adequate in computational terms. Therefore, a learning algorithm [14] is applied to the set of observed patterns. It has two main objectives : (1) to generalize the operator definition for patterns not observed in the sample, and (2) to reduce the representation cost of the operator. In this paper we use the ISI algorithm [4] that meets both objectives. ISI receives as input a collection of examples  $(X, y)$  and outputs a collection of intervals that completely describes a  $W$ -operator  $\psi$  and which is consistent with the input data, i.e.,  $\psi(X) = y$  for each input pair  $(X, y)$ .

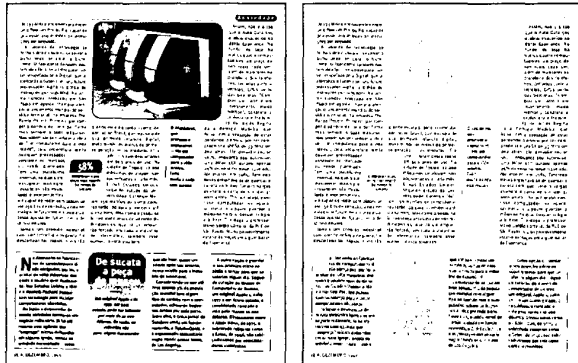


Figure 2: A test page and the result of the designed operator.

Once an operator  $\Psi_1$  is designed from pairs  $(S, I)$  of sample images, a second operator  $\Psi_2$  may be designed from pairs  $(\Psi_1(S), I)$ , a third one from pairs  $(\Psi_2(\Psi_1(S)), I)$  and so on. The composed operator  $\Psi_2\Psi_1$  is called a two-iteration operator. Analogously,  $\Psi_3\Psi_2\Psi_1$  is called a three-iteration operator. Effectiveness of iterated operators has been investigated for the case of increasing operators in [15], and for the class of (not necessarily increasing)  $W$ -operators in [16].

#### 4 Experimental Results

The automatic design technique described above was applied to segment text areas from pages of two sets of page images. Training images like those shown in Fig. 1 were used to design the operators. The images were obtained in high resolution (200 and 300 dpi, respectively), binarized by a simple threshold operation, and down-sampled to get images with resolution equivalent to 100dpi. The operators were trained to segment only black characters (in a white background), and only those with standard font size. Since the expected result from the segmentation (ideal image) is a subset of the observed image, we designed anti-extensive operators (all elements of the kernel contains the origin  $o$ ).

For the first set of images, a two-iteration operator  $\Psi = \Psi_2\Psi_1$  were designed using a total of 5 pairs of training images. Letting  $(S_1, I_1), \dots, (S_5, I_5)$  denote the training pairs of images, the first iteration operator,  $\Psi_1$ , were designed from  $(S_1, I_1), \dots, (S_4, I_4)$  over the  $7 \times 5$  window, while the second one,  $\Psi_2$ , were designed from  $(\Psi_1(S_2), I_2), \dots, (\Psi_1(S_5), I_5)$  over a 21-point window (the  $5 \times 5$  window without the four corner points). Figure 2 shows the result of  $\Psi$  applied on a test page.

Text objects of standard font size are kept almost as they were in the image before the processing, while

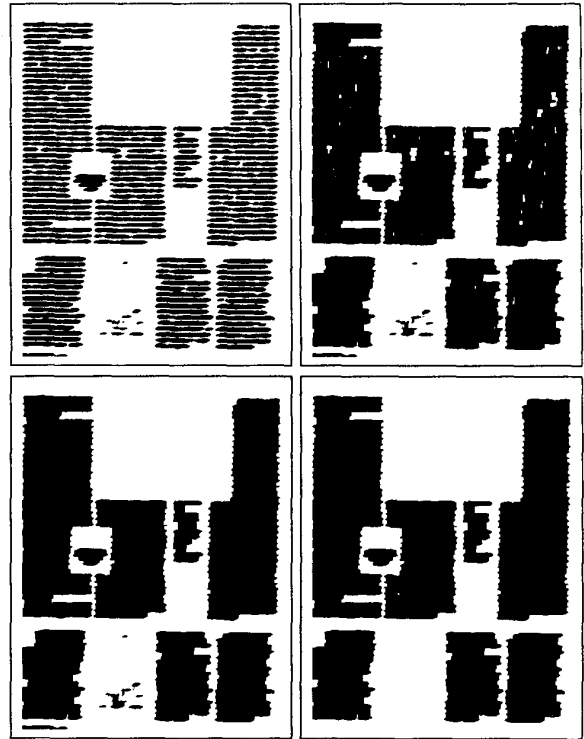


Figure 3: Effects of the post-processing procedure. From left to right, from top to bottom: results of the order filter, of the vertical closing, of the closing of holes, and of the area open, respectively.

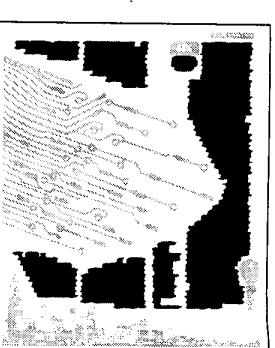
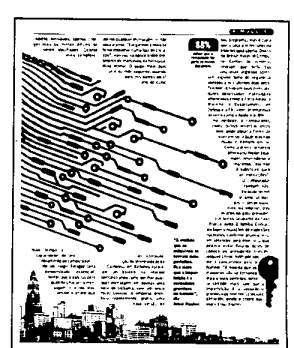
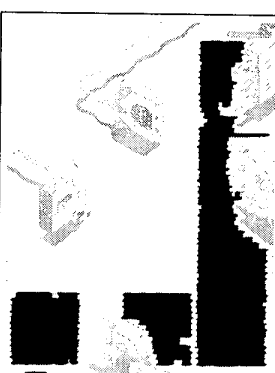
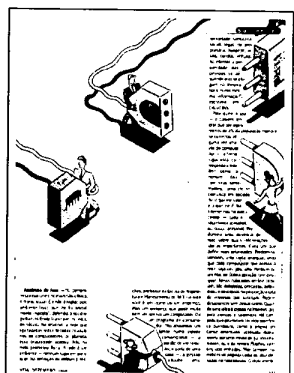
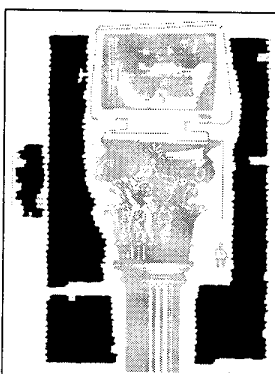
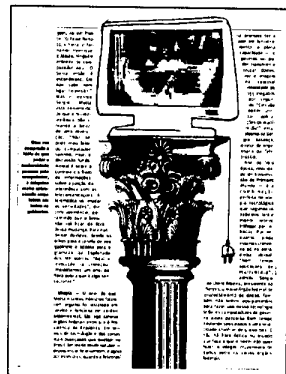
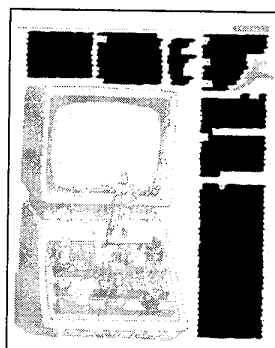
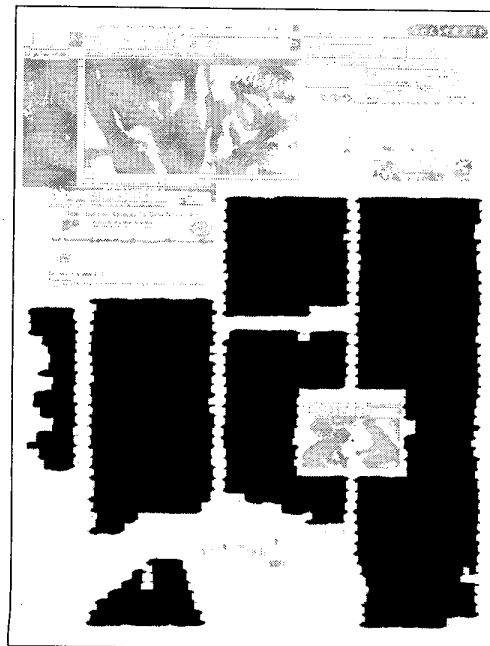
non-text objects and text of non-standard font size are almost completely removed. Note that the density of pixels in the area corresponding to text objects is much larger than in non-text areas. Based on this fact, a post-processing procedure consisting of the following sequence of filters is applied :

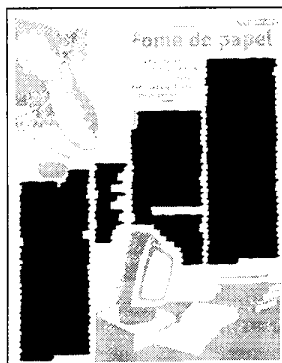
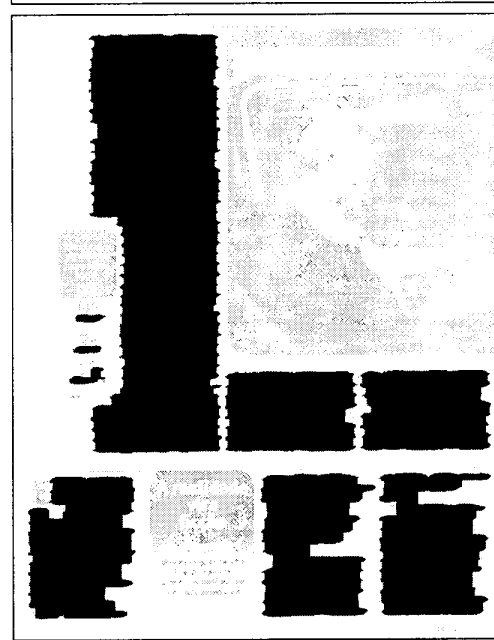
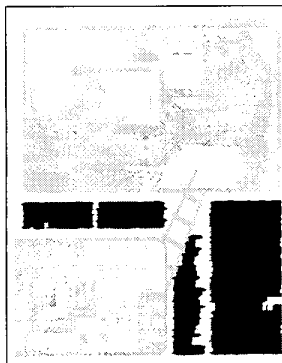
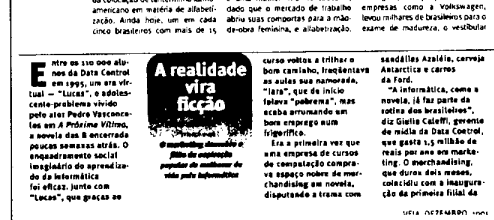
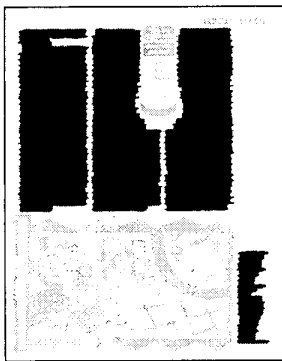
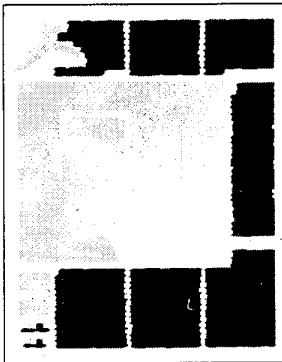
- a 18-order filter, relative to the  $7 \times 20$  window,
- a closing by a vertical line structuring element of length 10,
- the closing of holes operator,
- an area open filter.

The parameters of the order filter and of the closing were empirically adjusted for the whole set of images, while the parameters of the area open filter were adjusted for each page. Figure 3 shows the effect of the post-processing sequence of filters applied on the result shown in Fig. 2.

Next we show several test images (of the first group) and respective segmentation results obtained applying

the designed operator plus the post-processing procedure. For each pair, the first image is the original (observed image) while the second one is the respective segmentation result, superposed to the original image. Some pairs are shown in a larger scale for better visualization.

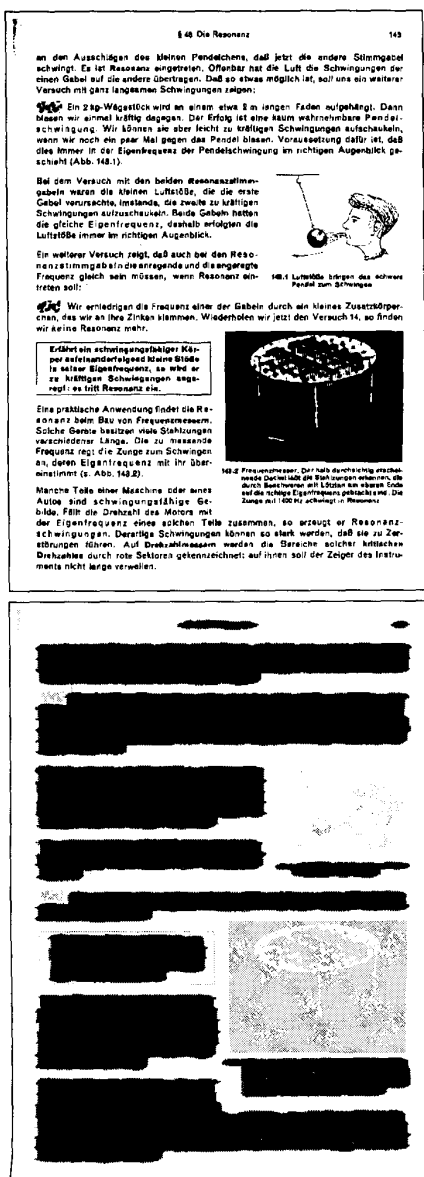




In all these pages, only few errors were verified. In one of the pages, the page number was missed by the post-processing procedure, because the object was smaller than other non-desired components removed by the area open filter. Some text in italic font were not segmented because they were not present in the training images.

The second set of images was obtained from a different source. The images in this set have, in general, a more complex layout than the ones in the first set.

For instance, they include mathematical formulas and their figures contain text of standard size. For this set, a three-iteration operator has been designed using a total of 8 pairs of training images, over the  $7 \times 5$ ,  $5 \times 5$  and 21-point (the  $5 \times 5$  window without the four corner points) windows, respectively. For the first-iteration operator, 6 pairs of training images were used, while for the last two iterations all 8 pairs were used. The same post-processing procedure described before, with the same parameter values, was applied to the resulting images. Next we show the segmentation result for some test pages of the second set.



**148 Die Resonanz**

an dem Aussehen des kleinen Pendelstahls, daß jetzt die andere Schwingung auftritt. Es ist Resonanz eingetreten. Offenbar hat die Luft die Schwingungen der einen Gabel auf die andere übertragen. Dafür so etwas möglich ist, sollte uns ein weiterer Versuch mit ganz langsamem Schwingungen zeigen:

**149.** Ein 24g-Wägstäbchen wird an einem etwa 8 m langen Faden aufgehängt. Dann lassen wir einmal kräftig dehnen. Der Erfolg ist eine kaum wahrnehmbare Pendelschwingung. Wir können es aber leicht zu trügerischen Schwingungen ausspielen, wenn wir noch einmal nach dem Dehnen blähen. Voraussetzung dafür ist, daß dies immer in der Eigenfrequenz der Pendelschwingung im richtigen Augenblick geschieht (Abb. 148.).

Bei dem Versuch mit den beiden **Resonanzpendeln** waren die kleinen Löffelöhrchen, die die erste Gabel verursachte, inständig, die zweite zu kräftigen Schwingungen befähigt. Beide Gabeln hatten die gleiche Eigenfrequenz, doch erst erfolgten die Löffelöhrchen immer im richtigen Augenblick.

Ein weiterer Versuch zeigt, daß auch bei den Resonanzschwingungen beide entsprechend die angegebene Frequenz gleich sein müssen, wenn Resonanz auftreten soll:

**150.** Wir erhöhen die Frequenz einer der Gablen durch ein kleines Zusatzdrehen, das wir an ihren Zinken klammern. Wiederholen wir jetzt den Versuch 14, so finden wir keine Resonanz mehr.

**Erklären Sie schwingungsfähige Körper aufeinanderfolgend kleine Blätte in ein Blatt! Resonanz, so wird er zu hören. Schwingt er nicht, so regt es mit Resonanz sie.**

Eine praktische Anwendung findet die Resonanz beim Bau von Frequenzmessern. Solche Geräte besitzen viele Stahlzungen verschiedener Länge. Die zu messende Frequenz wird auf die gleichen Schwingungen, an deren Eigenfrequenz mit ihr übereinstimmt (s. Abb. 149.B).

Manche Teile einer Maschine oder eines Autos sind schwingungsfähige Gebilde. Fällt die Drehzahl des Motors mit der eigenen Frequenz eines Teiles zusammen, so erzeugt er Resonanzschwingungen. Derselbe Schwingungen können so stark werden, daß sie zu Zerstörungen führen. Auf Drehzahlemessen werden die Bereiche solcher kritischen Drehzahlen durch rote Sektoren gekennzeichnet; auf ihnen soll der Zeiger des Instruments nicht lange verweilen.

**151 Messung der elektrischen Stromstärke**

Fließt in der Zeit  $t$  die Ladung  $Q$  durch einen Querschnitt des Leiters, so berechnet man die Stromstärke  $I$  als Quotient aus der Ladung  $Q$  und der Zeit  $t$ :

$$I = \frac{Q}{t} \quad (151)$$

Die Einheit der elektrischen Stromstärke ist 1 Ampere (A). Unter 1 A versteht man die Stromstärke, bei der 1 Coulomb in 1 s durch einen Querschnitt des Leiters fließt.

Nach § 95 bedeutet dies:

Ein Strom der Stärke 1 Ampera akkumuliert 0,74 cm³ Knaufgas in 1 s ab bei 0 °C und 760 Torr oder 1,18 mg Gold in 1 s:

$$1 A = 1 \frac{cm^3}{s} \quad (151.2)$$

$$1mA (Milliampere) = 1 \frac{m}{s} \quad (151.3)$$

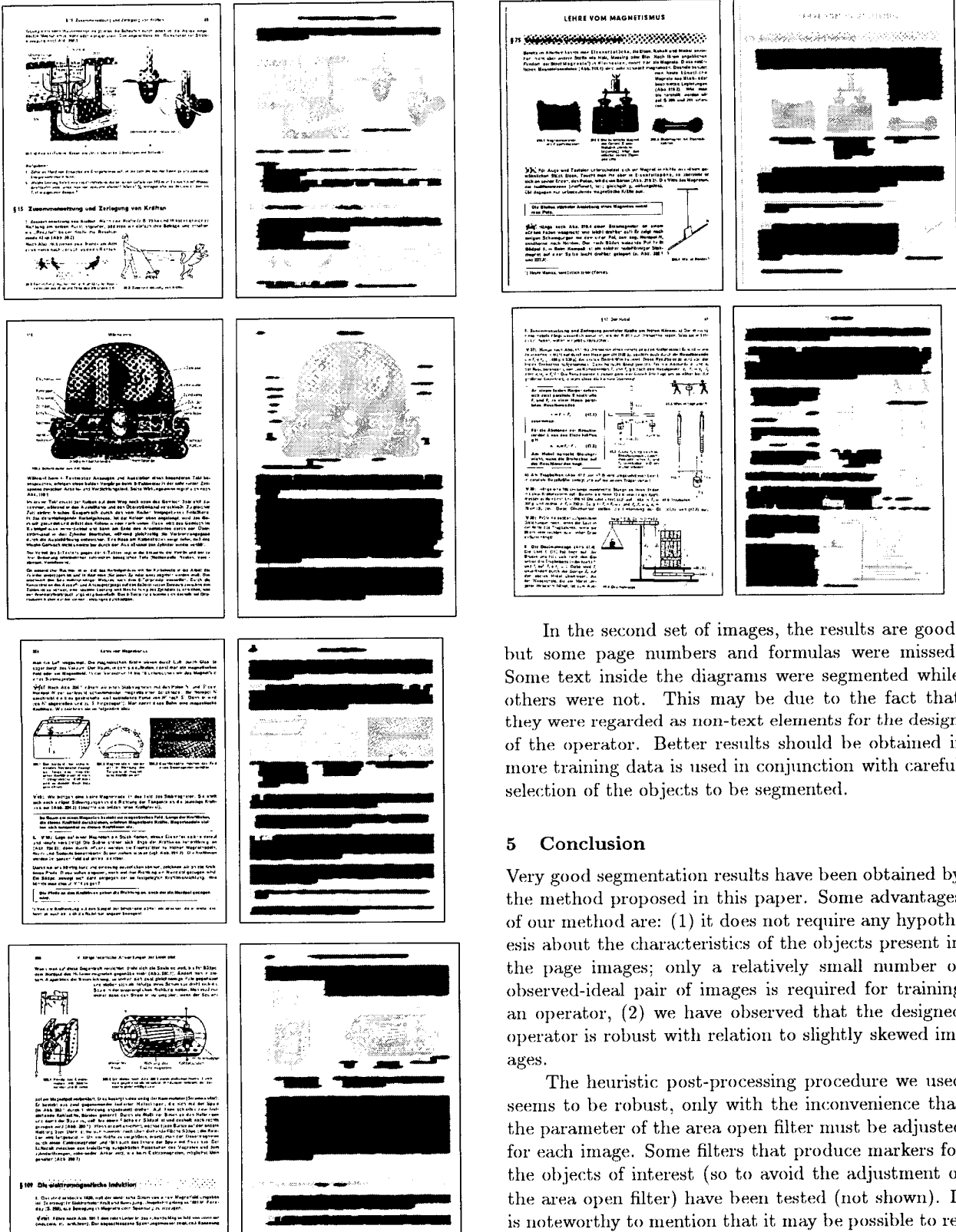
Fließt 100 g in 1 s, so ist die Stromstärke  $I = Q/t = 10 \text{ C} / 1 = 5 \text{ C/s} = 5 \text{ A}$ . Mit 20 s Muß bei diesem Strom die Ladung

$$Q = I \cdot t = 5 \cdot 20 = 100 \text{ C} \quad (151.4)$$

Z. Bei einer bestimmten Stromstärke  $I_0$  ist die doppelte bzw. dreifache Zeit die doppelte bzw. dreifache Ladung. Der Quotient  $Q/t = 2/2 = 3/3$  bleibt konstant. Bei größerer Stromstärke fließt deponier in gleicher Zeit mehr Ladung. Der Strom entwickelt dann auch je Sekunde mehr Wärme und die stärkere magnetische Wirkung aus. Da sich der Hinderniswiderstand verzögert, kann man das Geschwindigkeitsverhältnis  $v$  in Amperen-Coulomben-Gleichung nicht mehr als Strommesser verwenden. Das gleiche gilt für Maßgeräte auf magnetischer Grundlage (§ 94):

Die Geschwindigkeit eines Gitters, eines Kreisels, eines Pendels usw. ist proportional mit der magnetischen Stromstärke, ein konstanter Faktor bestimmt. Obwohl Gitter, Kreisel usw. die gleiche Zeit  $t$  für die gleichen Ladungen  $Q$  durchflossen, abhängt von der Reihenfolge. Die Stromstärke  $I = Q/t$  ist in ihrem gleich; die Angabe der Instrumente kann also an der Geschwindigkeit nachgeprüft werden. Ein Strommesser gestaltet mit dem Geschwindigkeitsverhältnis zu einem Maßgeräte, das man Ladung und Zeit direkt bestimmt. Dies entzieht dem Tachymeter im Auto, das ohne Messung von Weg ( $s$ ) und Zeit ( $t$ ) die Geschwindigkeit  $v = s/t$  unmittelbar anzeigt.

Im unverzweigten Stromkreis ist die Stromstärke überall gleich groß.



place the post-processing procedure by automatic designed operators, eliminating at all the need for adjusting the parameters of the post processing procedure. This is one of the issues for future research.

Another issue we would like to investigate further is the appropriate resolution of the images. When documents are to be processed by OCRs they are usually scanned at a relatively high resolution (300dpi or more). Since time to process an image is also proportional to the image size, a way to cut down the processing time is to use low resolution images. In our approach, we have used images of resolution approximately 100dpi, and one of our next goals is to investigate the application of the method on images of lower resolutions.

## 6 Acknowledgements

N. S. T. Hirata acknowledges support from FAPESP (process 98/14328-6).

## References

- [1] T. Pavlidis. Page Segmentation and Classification. *CVGIP: Graphical Models and Image Processing*, 54(6):484–496, November 1992.
- [2] K. Kise, A. Sato, and M. Iwata. Segmentation of Page Images Using the Area Voronoi Diagram. *Computer Vision and Image Understanding*, 70(3):370–382, June 1998.
- [3] A. Antonacopoulos. Page Segmentation Using the Description of the Background. *Computer Vision and Image Understanding*, 70(3):350–369, June 1998.
- [4] J. Barrera, E. R. Dougherty, and N. S. Tomita. Automatic Programming of Binary Morphological Machines by Design of Statistically Optimal Operators in the Context of Computational Learning Theory. *Electronic Imaging*, 6(1):54–67, January 1997.
- [5] J. Barrera, R. Terada, R. Hirata Jr, and N. S. T. Hirata. Automatic Programming of Morphological Machines by PAC Learning. *Fundamenta Informaticae*, 41(1-2):229–258, January 2000.
- [6] J. Barrera, R. Terada, F. S. C. da Silva, and N. S. Tomita. Automatic Programming of Morphological Machines for OCR. In *Mathematical Morphology and its Applications to Image and Signal Processing*, pages 385–392, Atlanta, GA, May 1996. International Symposium on Mathematical Morphology, Kluwer Academic Publishers.
- [7] J. Barrera, R. Terada, R. A. Lotufo, N. S. T. Hirata, R. Hirata Jr., and F. A. Zampirolli. An OCR based on Mathematical Morphology. In *Nonlinear Image Processing IX*, volume 3304 of *Proceedings of SPIE*, pages 197–208, San Jose, CA, January 1998.
- [8] J. Barrera, G. J. F. Banon, R. A. Lotufo, and R. Hirata Jr. MMach: a Mathematical Morphology Toolbox for the Khoros System. *Electronic Imaging*, 7(1):174–210, 1998.
- [9] P. Salembier and J. Serra. Flat Zones Filtering, Connected Operators, and Filters by Reconstruction. *IEEE Transactions on Image Processing*, 4(8):1153–1160, August 1995.
- [10] J. Serra. *Image Analysis and Mathematical Morphology*. Academic Press, 1982.
- [11] H. J. A. M. Heijmans. *Morphological Image Operators*. Academic Press, Boston, 1994.
- [12] P. Soille. *Morphological Image Analysis*. Springer-Verlag, Berlin, 1999.
- [13] E. R. Dougherty. *Random Processes for Image and Signal Processing*. SPIE and IEEE Presses, Bellingham, 1998.
- [14] T. M. Mitchell. *Machine Learning*. McGraw-Hill Series in Computer Science. McGraw-Hill, March 1997.
- [15] E. R. Dougherty, Y. Zhang, and Y. Chen. Optimal Iterative Increasing Binary Morphological Filters. *Optical Engineering*, 35(12):3495–3507, December 1996.
- [16] N. S. T. Hirata, E. R. Dougherty, and J. Barrera. Iterative Design of Morphological Binary Image Operators. *to appear*, 2000.